Staging of tau distribution by positron emission tomography may be useful in clinical staging of Alzheimer disease

Staging of tau distribution by positron emission tomography may be useful in clinical staging of Alzheimer disease

Kenta Aohara, Shinobu Minatani, Hiroko Kimura, Jun Takeuchi, Akitoshi Takeda, Joji Kawabe, Yasuhiro Wada, Aya Mawatari, Yasuyoshi Watanabe, Hitoshi Shimada, Makoto Higuchi, Tetsuya Suhara, Yoshiaki Itoh

Self-Archiving by Author(s)

Placed on: Osaka City University Repository

Neurology and Clinical Neuroscience

ORIGINAL ARTICLE

Staging of tau distribution by positron emission tomography may be useful in clinical staging of Alzheimer disease

Kenta Aohara[1], Shinobu Minatani[1], Hiroko Kimura[1], Jun Takeuchi[1], Akitoshi Takeda[1], Joji Kawabe[2], Yasuhiro Wada[3], Aya Mawatari[3], Yasuyoshi Watanabe[3], Hitoshi Shimada[4], Makoto Higuchi[4], Tetsuya Suhara[4], Yoshiaki Itoh[1]

[1]Department of Neurology and [2]Department of Nuclear Medicine, Osaka City University Graduate School of Medicine, Osaka, Japan;
[3]RIKEN Center for Biosystems Dynamics Research, Kobe, Japan;
[4]Department of Functional Brain Imaging Research (DOFI), Clinical Research Cluster, National Institute of Radiological Sciences (NIRS), National Institutes for Quantum and Radiological Science and Technology (QST), Chiba, Japan

Correspondence

Yoshiaki Itoh

Department of Neurology, Osaka City University Graduate School of Medicine, Asahicho 1-4-3, Abenoku, Osaka City, Osaka Prefecture, 545-8585, Japan

E-mail: y-itoh@med.osaka-cu.ac.jp

Short title

Staging of Alzheimer disease by Tau PET

Abstract

Background: Clinical staging of Alzheimer disease (AD) may help develop novel treatment in the early stage.

Aim: We measured the accumulation of amyloid beta (Aβ) and tau with positron emission tomography (PET) in patients with AD to explore its utility for clinical staging.

Methods: Six patients with AD, two patients with mild cognitive impairment (MCI), and 12 healthy controls (HC) were studied. Aβ and tau accumulation was evaluated with [11C]PiB and [11C]PBB3, respectively.

Results: PBB3-PET showed that two cases were in stage I-II (Braak stage), one case was in stage III-IV, and three cases were in stage V-VI. PiB-PET showed that all cases were in stage C. The duration of the disease correlated positively with PBB3 staging but not with PiB staging. The performance on the Mini-Mental State Examination (MMSE) tended to decrease with advancing of PBB3 stage but not with PiB stage. PBB3 SUVR and PiB SUVR in all AD signature areas including the parahippocampal gyrus were significantly higher in AD than in HC. A decrease in MMSE is correlated with increases in PBB3 and PiB. Increase in PBB3 started with decrease in MMSE whereas increase in PiB was already observed in the point of highest MMSE, indicating amyloid is already accumulated in the earliest stage.

Conclusions: The expansion of tau distribution from the parahippocampal gyrus to the cerebral cortex was observed with advancing AD, whereas Aβ distribution was already advanced in the earliest stage. PBB3 may be useful in determining stages in AD based on tau distribution.

Key words

amyloid PET, dementia, parahippocampal gyrus, PBB3, PiB,

Introduction

The classical amyloid hypothesis of Alzheimer disease (AD) suggests that polymerization of amyloid beta (Aβ) is the first step to the common pathway of neurodegeneration.[1] Tau accumulation and neuronal dysfunction may follow the Aβ accumulation.[2] However, this sequence was mainly confirmed in hereditary AD,[3] and little is reported on sporadic AD. We previously reported that a mild amount of tau accumulates age-dependently in healthy controls and may trigger robust Aβ accumulation and further tau accumulation in AD development.[4] Furthermore, the failure of many clinical trials targeting Aβ in already developed AD indicates that not Aβ but tau may be the main worsening factor after onset.[5] Thus, tau may be involved in the progress of AD and has become a novel target of AD treatment.[6]

The pathological accumulation of Aβ as well as neurofibrillary tangle (NFT) was suggested to spread from the limbic system to the neocortex, whereas few clinical data on such spread based on AD staging were reported.[7,8] Aβ is already accumulated at AD signature areas in early AD or even in mild cognitive dementia (MCI) due to AD.[9-11] The spreading pattern of Aβ has been scarcely reported along the stages of advancement of AD[9-11]. In addition to Aβ, we measured the accumulation of tau with a radiopharmaceutically significant tracer, 2-[(1E, 3E)-4-[6-[[11C] methylamino]

pyridin-3-yl]buta-1,3-dien-1-yl]-1,3-benzothiazol-6-ol ([11C]PBB3), for positron emission tomography (PET)[12-14] in patients with various durations of AD and judged the stage of tau distribution based on the standard pathological staging by Braak.[7]

Materials and Methods

Ethical approval. All procedures performed in studies involving human participants were approved by the Institutional Research Ethics Committee of Osaka City University Graduate School of Medicine (IRB# 3009 and 1735) and were in accordance with the 1964 Helsinki declaration and its later amendments.

Informed consent. Written informed consent was obtained from all participants or from close family when the participants were cognitively impaired.

Healthy Controls. Healthy controls (HC) without history of brain disorders or subjective abnormality were openly recruited as candidates. A board-certified neurologist interviewed them and obtained detailed medical histories including alcohol consumption. All candidates took physical examination covering vital and cardiopulmonary systems. Thorough neurological examinations, including general

cognitive function tests, were performed by the same neurologist. The Mini-Mental State Examination (MMSE) and the revised Hasegawa Dementia Scale (HDS-R) were scored by qualified clinical psychologists (MA, NK). Blood samples were collected to evaluate general physical condition, including thyroid function and vitamin B1. Magnetic resonance images (MRIs) were also evaluated.

The exclusion criteria were as follows: 1) history of any brain diseases, brain surgery, or head trauma requiring hospitalization; 2) high risk for cerebrovascular diseases, including poorly controlled diabetes, dyslipidemia, and high blood pressure above the recommended level of standard guidelines; 3) any neurological findings suggesting brain disorders; 4) cognitive test [MMSE, HDS-R, and RBMT (Rivermead Behavioral Memory Test)] indicating border-zone or worse level; and 5) MRI lesions including asymptomatic lacunas (less than 15mm in diameter, high in T2, FLAIR and low in T1), severe white matter lesion (more than 1 in Fazekas grade[15]), more than 4 cerebral microbleeds, and atrophy beyond average for their age by visual inspection; and 6) amyloid PET imaging was employed for the exclusion of enrollment. No other biomarkers were examined in the HC group.

AD and MCI. Cases with AD and MCI due to AD were recruited from patients attending

the outpatient clinic of Osaka City University Hospital. Medical history, neurological findings and general blood tests were evaluated by neurologists specializing in dementia. MMSE and HDS-R were scored by qualified clinical psychologists. An MRI of the brain including coronal section was taken.

The diagnostic criteria of MCI due to AD by the National Institute on Aging-Alzheimer's Association workgroups was employed for the diagnosis of MCI.[16] To better understand the role of tau compared with Aβ in the development of AD, MCI was diagnosed regardless of the findings of amyloid PET imaging. For the diagnosis of AD, IWG-2 criteria for typical AD was employed with amyloid PET as an in vivo evidence of AD pathology.[17] Apparent familial AD was not included in the present study.

The same exclusion criteria applied for HC were applied for AD and MCI to exclude confounding diseases such as diabetes, dyslipidemia and hypertension.

Disease duration of AD was defined as a period from the onset of dementia to the time of the present imaging study. The onset was determined as a converting time in case of MCI or retrospectively speculated at the initial visit for early AD. No cases without proper medical records on the onset were involved.

PET data acquisition. [11C]PBB3 and [11C]Pittsburgh compound-B (2-[4-([11C]

methylamino) phenyl]-1,3-benzothiazol-6-ol, [11C]PiB) were produced based on previously reported methods.[13,18,19] [11C]PBB3-and [11C]PiB-PET images were acquired with a Siemens Biograph16 scanner (Siemens/CTI, Knoxville, TN, USA) and with an Eminence-B PET scanner (Shimadzu Co., Kyoto, Japan), respectively. For tau imaging, [11C]PBB3 in the range of 370 MBq (body weight ≤ 50 kg) to 555 MBq (body weight ≥70 kg) was intravenously injected to the patient in a dimly lit room to avoid photoracemization. A 60-minute PET scan was performed in the list mode. The acquired data were sorted into dynamic data of 6×10 s, 3×20 s, 6×60 s, 4×180 s, and 8×300 s frames. For Aβ imaging, each subject received 400 to 500 MBq of [11C]PiB intravenously over 1 minute. After the injection, a static scan image acquisition was performed for 50 to 70 minutes. PET images for [11C]PBB3 and [11C]PiB were reconstructed by filtered back projection using a 4-mm full width at half maximum (FWHM) Hanning filter and a 5-mm FWHM gaussian filter with attenuation and scatter correction, respectively.

MRI acquisition. The MRI data were obtained with a 1.5- or 3-Tesla magnetic resonance scanner (MAGNETOM Avanto, Siemens Healthcare, Erlangen, Germany or Ingenia, Philips Healthcare, Best, The Netherlands). Three-dimensional volumetric acquisition of a T1- weighted gradient echo sequence (repetition time range/echo time range, 6.5

ms/3.2 ms; field of view [frequency × phase], 240 mm×240 mm; matrix, 256×256;

contiguous axial slices of 1.5 mm thickness) was performed.

Image processing. All images were processed using PMOD software version 3.7 (PMOD

Technologies Ltd., Zurich, Switzerland)[20] and Statistical Parametric Mapping software

(SPM12, Wellcome Department of Cognitive Neurology, London, UK), operating on the

MATLAB software environment (version R2016b; MathWorks, Natick, MA, USA)[21].

Acquired [11C]PBB3 and [11C]PiB images were transformed into standard brain using

PMOD, and then SUVR images were generated with the cerebellar cortex as a reference

region using the frame summation of dynamic image for 30 to 50 minutes after

[11C]PBB3 injection and for 50 to 70 minutes after [11C]PiB injection. The SUVR level of

each volume of interest (VOI) was calculated in a manually set region of interest (ROI)

as shown in Online Resource 1.

Each T1-weight MRI was segmented and anatomically normalized to MNI152

standard space (Montreal Neurological Institute, Montreal, QC, Canada) using SPM12

and Diffeomorphic Anatomical Registration Through Exponentiated Lie Algebra

(DARTEL) [22]. The [11C]PBB3 SUVR and [11C]PiB SUVR images were co-registered to

individual T1-weighted MRI using PMOD and then normalized to MNI space using the

same parameters as those for MRI (flow fields method) with smoothing at 8-mm

full-width-at-half-maximum.

Criteria for Aβ accumulation. Aβ accumulation was visually evaluated based on the

Japanese Alzheimer's Disease Neuroimaging Initiative (J-ADNI) Visual Criteria for

[11C]PiB-PET (J-ADNI_PETQC_Ver1.1) modified from ADNI PET core criteria [23]. The

four regions selected for the assessment were the precuneus combined with posterior

cingulate gyrus, frontal lobe, lateral temporal lobe, and lateral parietal lobe. When the

accumulation in one of the four cerebral cortices was higher than that in the white

matter just below the cortex, the case was determined as positive. When none of the

four cortices had higher accumulation than the white matter, the case was confirmed as

negative.

Voxel-wise analysis of [11C]PBB3 and [11C]PiB. A voxel-wise comparison of [11C]PBB3

and [11C]PiB accumulation data was performed between individual AD cases and the

HC group by single subject analysis using SPM12.[24] Age was included as a covariate.

The threshold for significance was set at $P < 0.05$ family-wise error (FWE)-corrected at

cluster level following $P < 0.01$ uncorrected at voxel level.

Regional SUVR and cognitive impairment in AD. In each ROI, regional SUVR was compared between HC and AD with a Mann-Whitney U-test, and the significance level was 5 %, two-tailed test. In addition to each ROI, the non-weighted average SUVR in the AD signature regions (i.e., the lateral temporal cortex, frontal cortex, posterior cingulate gyrus, precuneus, and parietal cortex) was statistically compared between the two groups. The parahippocampal gyrus, which is pathologically known to have no or very limited accumulation of Aβ, was not included in the AD signature region.

The correlation between the SUVR and MMSE evaluated at the same time in AD was statistically evaluated in each ROI as well as in the averaged AD signature regions by the Spearman's rank correlation coefficient. $P < 0.05$ was regarded as statistical significance. Analyses were carried out using SPSS version 25 for windows (SPSS Inc., Chicago, IL, USA).

Results

Demographical data. Table 1 shows the demographical data of the AD, MCI, and HC groups. The age of patients in the AD group varied widely from 51 to 85 years old. Two patients with MCI were in their over 80 years of age. The age distribution of the HC

group was similar to that of the AD group [71.8 ± 8.7 years, mean ± standard deviation

(SD)]. In the AD group, either MMSE or HDS-R was below the cutoff level of dementia,

whereas subjects in the MCI and HC groups had little or no deduction of points on the

cognitive tests.

Braak's staging. In each patient with AD, PBB3 as well as PiB accumulation was

statistically compared with that of the HC group by the statistical parametric mapping

method. Stage of PBB3 and PiB distribution was determined based on the pathological

stage of NFT and amyloid, respectively, by Braak (Fig 1). The PBB3-PET study showed

that two cases were in stage I-II (transentorhinal stage), one case was in stage III-IV

(limbic stage), and three cases were in stage V-VI (isocortical stage); whereas, PiB-PET

showed that all cases were in stage C (neocortical stage) (Table 1).

The duration of the disease correlated positively with PBB3 staging but not

with PiB staging. MMSE tended to decrease with advancing of PBB3 stage, but not of

PiB stage (Fig 2).

Cognitive deterioration and tau/ amyloid beta

PBB3 SUVR and PiB SUVR in all AD signature regions as well as the parahippocampal

gyrus were significantly higher in the AD group than in the HC group ($P < 0.05$) (Fig 3).

The decrease in MMSE was statistically significantly correlated with the increase in

PiB ($P < 0.05$). A similar tendency was found in the decrease in MMSE and increase in

PBB3, without statistical significance.

Of note is that the linear correlation between the decrease in MMSE and

increase in PBB3 crossed the basal point, namely the SUVR level of the HC group,

whereas the linear correlation between the decrease in MMSE and increase in PiB

shifted higher and did not cross the basal point (Fig 3), indicating that amyloid is

already widely distributed in the earliest stage of AD. The shift in PiB was not observed

in the parahippocampal gyrus.

Discussion

In the present PET study, expansion of tau distribution from the

transentorhinal cortex to the cerebral cortex was observed with advancing cognitive

severity of AD, whereas Aβ distribution was already advanced in the earliest stage.

These results suggest that PBB3 may be useful in determining stages in AD based on

tau distribution, whereas PiB is helpful in early diagnosis of AD.

Similar report supporting our data has been recently published by Jack et al[25]. They also reported two steps in developing AD; i.e. first Aβ accumulation and later tau. However they failed to analyze spatial development of the pathological changes we reported in the present study.

We previously reported that tau accumulates with age in the region related to AD.[4] This is in good accordance with the previous reports by Jagust WJ et al. regarding [18F]AV1451.[26] In the present study, we found further accumulation of tau in accordance with cognitive deterioration, starting from the transentorhinal cortex and extending into neocortex.

A clinicopathological study already reported that MMSE was significantly correlated with NFT and neuron number but not with amyloid volume in CA1, the entorhinal cortex, and area 9.[27] NFT and neuronal loss but not senile plaque in superior temporal sulcus were correlated with disease severity.[28] Using novel tau tracer [18F]AV1451 and classical Aβ tracer [18F]AV45, tau accumulation was strongly correlated and Aβ was only mildly correlated with cognitive decline in AD.[29] These reports are quite consistent with the present findings that Aβ is already accumulated in the earliest stage of AD and continues to accumulate slowly thereafter.

A recent pathological analysis also reported widespread but exclusive cortical

distribution of Aβ in the earliest stage of AD.[30] Utilizing the North American

Alzheimer's Disease Neuroimaging Initiative (ADNI) cohort, Palmqvist et al. reported

that the earliest accumulation of Aβ was found within the default-mode network,

including the posterior cingulate cortex, the precuneus, and the medial orbitofrontal

cortex.[31] The accumulation became widespread before the onset of dementia.[31] Using

the same ADNI data with tau PET by [18F]AV1451, Tosun et al. reported that early tau

deposition was found in the inferior temporal and inferior parietal regions.[32] The

further deposition pattern varied with different cognitive performance and clinical

outcome measures.[32] These reports are in good agreement with the present findings

that the spread of tau reflects cognitive deterioration in typical AD cases.

One of the drawbacks of [11C]PBB3 is that it accumulates at the cerebral

sinuses including the superior sagittal sinus and transverse sinus. The extent of

accumulation varies between cases. Low accumulation can be eliminated by masking

the accumulation at the sinuses, although high accumulation can affect apparent

measurement of the cerebral cortex. In the present study, high accumulation

neighboring the superior sagittal sinus and transverse sinus in the occipital lobe was

considered as artifact.

The limited dynamic range of [11C]PBB3 to detect tau accumulation also may

overlook smaller lesion or milder accumulation.[14] In the present study, increase in

[11C]PBB3 accumulation at the parahippocampal gyrus and lateral temporal cortex, the

regions usually involved in the earliest stage, was not detected in a case with AD.

Possible overestimation of the aging effect on tau accumulation at these regions may

additionally reduce the significance[4]. Further development of a more sensitive tracer is

warranted.

Pathology was not confirmed in any case in the present study. There might be

some gap between [11C]PBB3 accumulation and pathological changes. Although the

distribution of tau by [11C]PBB3 in AD in the present study is consistent with the

distribution of lesions in the previous pathological reports, further pathological

confirmation is warranted. A greater number of subjects with AD should be studied to

draw definite conclusions.

Conflict of Interest: Authors H.S., M.H., and T.S. possess patent royalty of PBB3.

References

1.   Selkoe DJ. The molecular pathology of Alzheimer's disease. *Neuron* 1991;**6**:487-98.

2.   Lemere CA, Lopera F, Kosik KS*, et al.* The E280A presenilin 1 Alzheimer mutation

produces increased Aβ42 deposition and severe cerebellar pathology. *Nature Medicine* 1996;**2**:1146.

3.   Bateman RJ, Xiong C, Benzinger TLS*, et al.* Clinical and Biomarker Changes in Dominantly Inherited Alzheimer's Disease. *New England Journal of Medicine* 2012;**367**:795-804.

4.   Kikukawa T, Saito H, Hasegawa I*, et al.* Localized Accumulation of Tau without Amyloid-beta in Aged Brains Measured with 11[C]PBB3 and [11C]PiB Positron Emission Tomography. *Journal of Alzheimers Disease and Parkinsonism* 2017;**7**:6.

5.   Honig LS, Vellas B, Woodward M*, et al.* Trial of Solanezumab for Mild Dementia Due to Alzheimer's Disease. *N Engl J Med* 2018;**378**:321-30.

6.   Li C, Gotz J. Tau-based therapies in neurodegeneration: opportunities and challenges. *Nat Rev Drug Discov* 2017;**16**:863-83.

7.   Braak H, Braak E. Neuropathological stageing of Alzheimer-related changes. *Acta Neuropathol* 1991;**82**:239-59.

8.   Schwarz AJ, Yu P, Miller BB*, et al.* Regional profiles of the candidate tau PET ligand 18F-AV-1451 recapitulate key features of Braak histopathological stages. *Brain* 2016;**139**:1539-50.

9.   Grothe MJ, Barthel H, Sepulcre J, Dyrba M, Sabri O, Teipel SJ. In vivo staging of regional amyloid deposition. *Neurology* 2017;**89**:2031-8.

10.   Thal DR, Attems J, Ewers M. Spreading of amyloid, tau, and microvascular pathology in Alzheimer's disease: findings from neuropathological and neuroimaging studies. *J Alzheimers Dis* 2014;**42 Suppl 4**:S421-9.

11.   Veitch DP, Weiner MW, Aisen PS*, et al.* Understanding disease progression and improving Alzheimer's disease clinical trials: Recent highlights from the Alzheimer's Disease Neuroimaging Initiative. *Alzheimers Dement* 2018.

12.   Shimada H, Kitamura S, Shinotoh H*, et al.* Association between Abeta and tau accumulations and their influence on clinical features in aging and Alzheimer's disease spectrum brains: A [11C]PBB3-PET study. *Alzheimers Dement (Amst)* 2017;**6**:11-20.

13.   Maruyama M, Shimada H, Suhara T*, et al.* Imaging of tau pathology in a tauopathy mouse model and in Alzheimer patients compared to normal controls. *Neuron* 2013;**79**:1094-108.

14.   Ono M, Sahara N, Kumata K*, et al.* Distinct binding of PET ligands PBB3 and AV-1451 to tau fibril strains in neurodegenerative tauopathies. *Brain* 2017;**140**:764-80.

15.   Fazekas F, Chawluk JB, Alavi A, Hurtig HI, Zimmerman RA. MR signal abnormalities at 1.5 T in Alzheimer's dementia and normal aging. *AJR Am J Roentgenol* 1987;**149**:351-6.

16.   Jack CR, Jr., Albert MS, Knopman DS*, et al.* Introduction to the recommendations

from the National Institute on Aging-Alzheimer's Association workgroups on diagnostic guidelines for Alzheimer's disease. *Alzheimers Dement* 2011;**7**:257-62.

17.   Dubois B, Feldman HH, Jacova C*, et al.* Advancing research diagnostic criteria for Alzheimer's disease: the IWG-2 criteria. *Lancet Neurol* 2014;**13**:614-29.

18.   Kimura Y, Ichise M, Ito H*, et al.* PET Quantification of Tau Pathology in Human Brain with 11C-PBB3. *J Nucl Med* 2015;**56**:1359-65.

19.   Hashimoto H, Kawamura K, Igarashi N*, et al.* Radiosynthesis, photoisomerization, biodistribution, and metabolite analysis of 11C-PBB3 as a clinically useful PET probe for imaging of tau pathology. *J Nucl Med* 2014;**55**:1532-8.

20.   Choi WH, Um YH, Jung WS, Kim SH. Automated quantification of amyloid positron emission tomography: a comparison of PMOD and MIMneuro. *Annals of Nuclear Medicine* 2016;**30**:682-9.

21.   Gallivanone F, Della Rosa PA, Castiglioni I. Statistical Voxel-Based Methods and [18F]FDG PET Brain Imaging: Frontiers for the Diagnosis of AD. *Curr Alzheimer Res* 2016;**13**:682-94.

22.   Ashburner J. A fast diffeomorphic image registration algorithm. *Neuroimage* 2007;**38**:95-113.

23.   Jagust WJ, Bandy D, Chen K*, et al.* The ADNI PET Core. *Alzheimers Dement* 2010;**6**:221-9.

24.   Maass A, Landau S, Baker SL*, et al.* Comparison of multiple tau-PET measures as biomarkers in aging and Alzheimer's disease. *Neuroimage* 2017;**157**:448-63.

25.   Jack CR, Wiste HJ, Botha H*, et al.* The bivariate distribution of amyloid-beta and tau: relationship with established neurocognitive clinical syndromes. *Brain* 2019;**142**:3230-42.

26.   Schöll M, Lockhart Samuel N, Schonhaut Daniel R*, et al.* PET Imaging of Tau Deposition in the Aging Human Brain. *Neuron* 2016;**89**:971-82.

27.   Giannakopoulos P, Herrmann FR, Bussiere T*, et al.* Tangle and neuron numbers, but not amyloid load, predict cognitive status in Alzheimer's disease. *Neurology* 2003;**60**:1495-500.

28.   Gomez-Isla T, Hollister R, West H*, et al.* Neuronal loss correlates with but exceeds neurofibrillary tangles in Alzheimer's disease. *Ann Neurol* 1997;**41**:17-24.

29.   Koychev I, Gunn RN, Firouzian A*, et al.* PET Tau and Amyloid-beta Burden in Mild Alzheimer's Disease: Divergent Relationship with Age, Cognition, and Cerebrospinal Fluid Biomarkers. *J Alzheimers Dis* 2017;**60**:283-93.

30.   Thal DR, Rub U, Orantes M, Braak H. Phases of A beta-deposition in the human brain and its relevance for the development of AD. *Neurology* 2002;**58**:1791-800.

31.   Palmqvist S, Scholl M, Strandberg O*, et al.* Earliest accumulation of beta-amyloid

occurs within the default-mode network and concurrently affects brain connectivity. *Nat Commun* 2017;**8**:1214.

32.   Tosun D, Landau S, Aisen PS*, et al.* Association between tau deposition and antecedent amyloid-beta accumulation rates in normal and early symptomatic individuals. *Brain* 2017;**140**:1499-512.

Figure Legends

Figure 1. Representative cases for Braak's staging of NFT (a) and senile plaque (b). In each case with AD, PBB3 (a) as well as PiB (b) accumulation was statistically compared with that of HC by the statistical parametric mapping method. No case was classified as stage A or stage B in Braak's staging of amyloid distribution (b).

Figure 2. Disease duration and Mini-Mental State Examination (MMSE) score at each stage in patients with AD. (a), (b) indicate neurofibrillary change staging of PBB3, (c) and (d) indicate amyloid deposits staging of PiB.

Figure 3. Scatter plots show correlation between Mini-Mental State Examination (MMSE) and PBB3 SUVR (a, c) or MMSE and PiB SUVR (b, d) in AD signature regions on average (a, b) and parahippocampal gyrus (c, d). The dotted line shows the regression line in the AD group. Detailed data on the correlation in each ROI were shown in Online Resource 2 for PBB3 and Online Resource 3 for PiB.
1) Difference in PBB3 or PiB accumulation between AD group and HC group.
2) Correlation between MMSE and PBB3, PiB SUVR. n.s.: not significant.
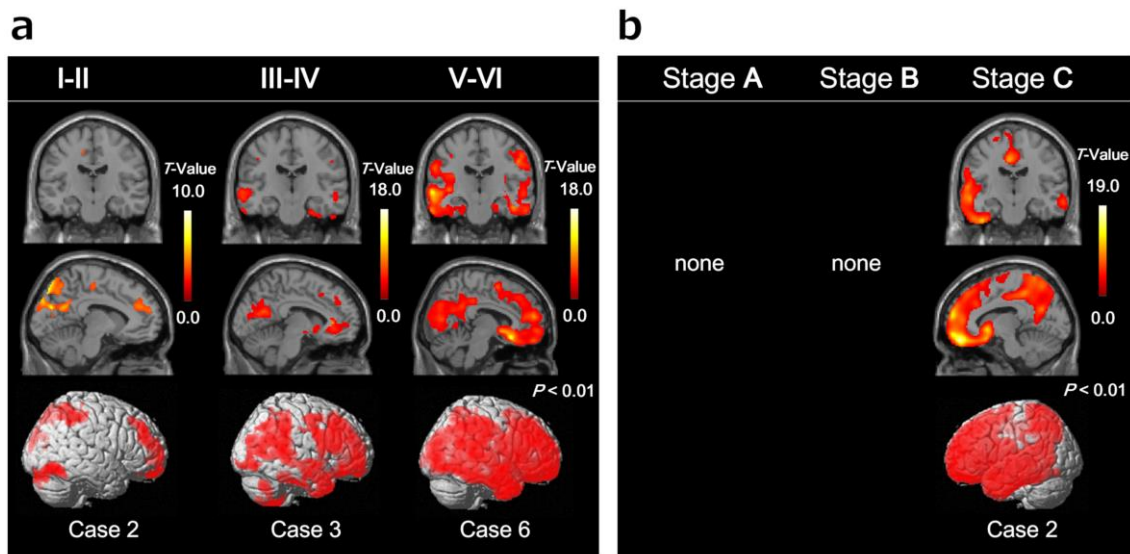
Figure 1. Representative cases for Braak's staging of NFT (a) and senile plaque (b). In each case with AD, PBB3 (a) as well as PiB (b) accumulation was statistically compared with that of HC by the statistical parametric mapping method. No case was classified as stage A or stage B in Braak's staging of amyloid distribution (b).
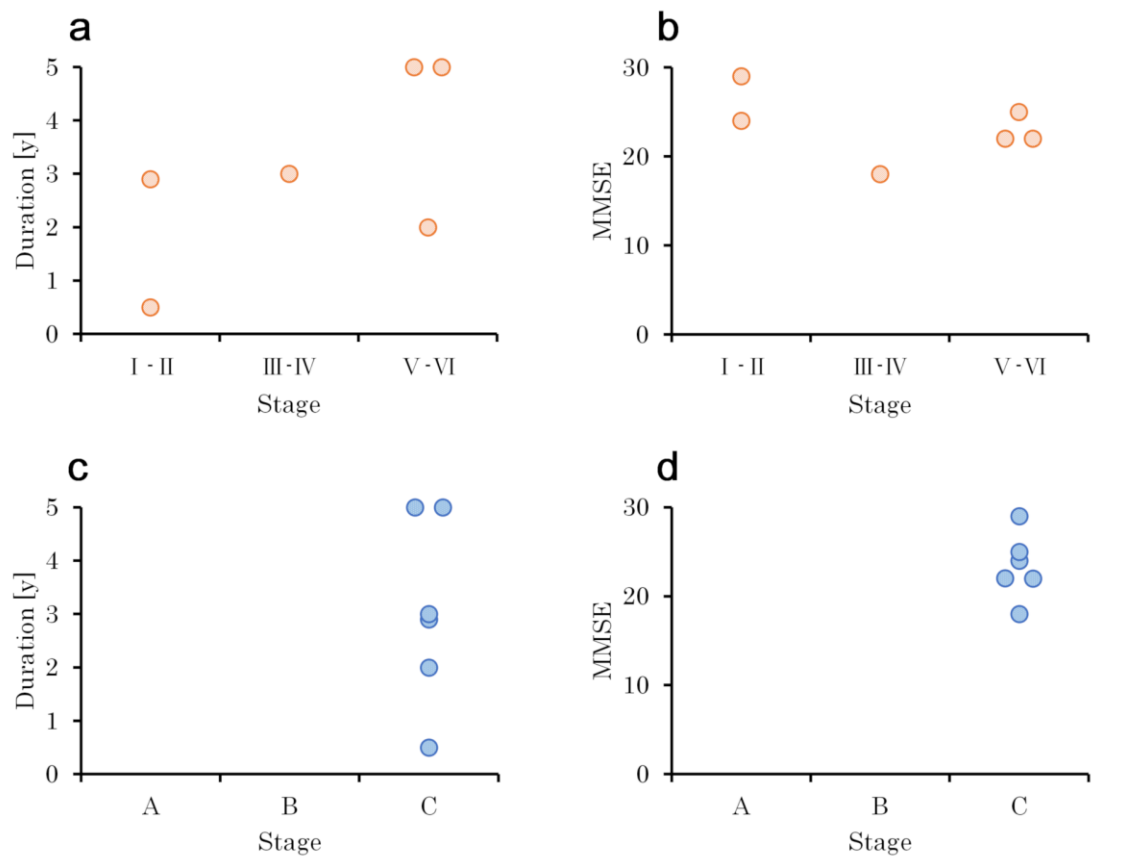
Figure 2. Disease duration and Mini-Mental State Examination (MMSE) score at each stage in patients with AD. (a), (b) indicate neurofibrillary change staging of PBB3, (c) and (d) indicate amyloid deposits staging of PiB.
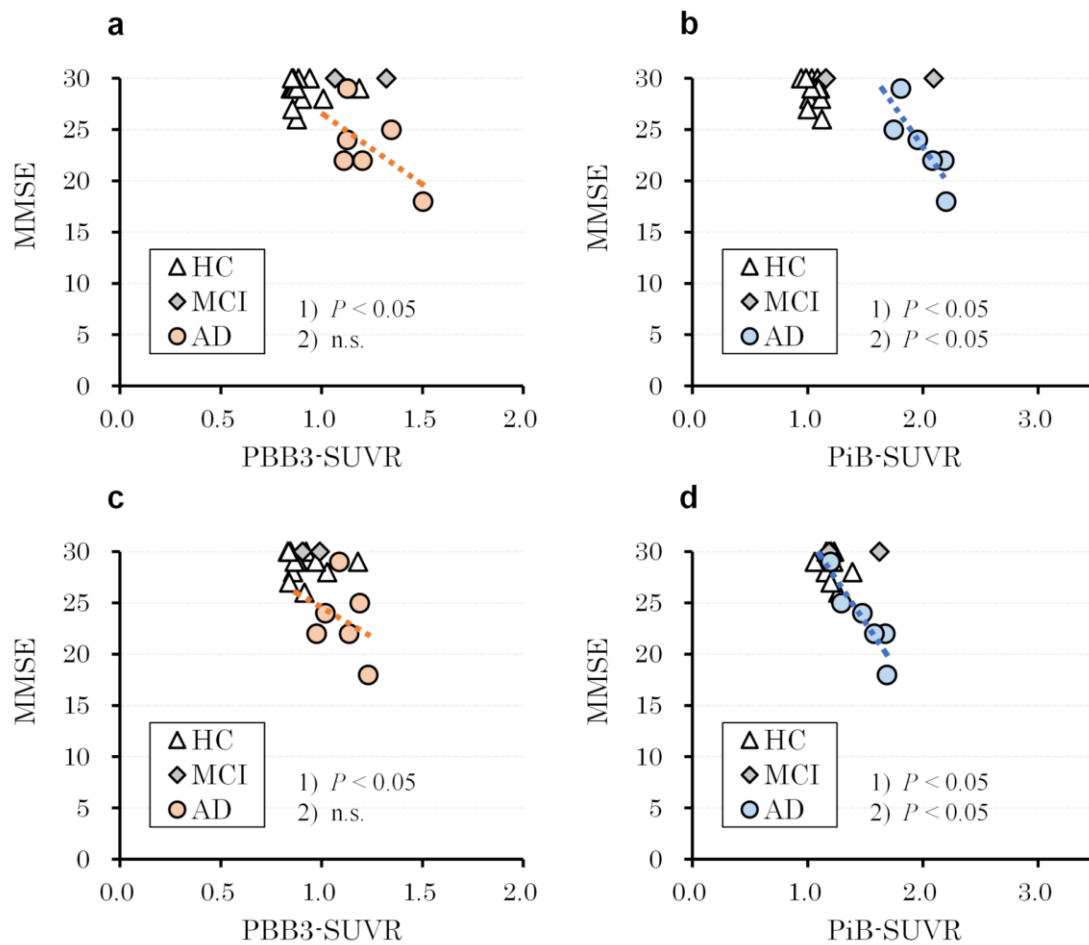
Figure 3. Scatter plots show correlation between Mini-Mental State Examination (MMSE) and PBB3 SUVR (a, c) or MMSE and PiB SUVR (b, d) in AD signature regions on average (a, b) and parahippocampal gyrus (c, d). The dotted line shows the regression line in the AD group. Detailed data on the correlation in each ROI were shown in Online Resource 2 for PBB3 and Online Resource 3 for PiB.

1) Difference in PBB3 or PiB accumulation between AD group and HC group.

2) Correlation between MMSE and PBB3, PiB SUVR. n.s.: not significant.

Table 1. Demographic data

Subject No.	Age	Gender	Disease Duration (y)	MMSE	HDS-R	Braak Stage PBB3	Braak Stage PiB
Alzheimer's Disease							
1	74	M	0.5	29	22	I-II	C
2	85	M	2.9	24	19	I-II	C
3	51	M	3.0	18	19	III-IV	C
4	70	F	5.0	25	24	V-VI	C
5	78	M	2.0	22	21	V-VI	C
6	60	F	5.0	22	27	V-VI	C
Mild Cognitive Impairment							
7	81	F	n.a.	30	30	I-II	Negative
8	82	M	n.a.	30	30	III-IV	C
Healthy controls							
n=12	$71.8 \pm 8.7^{\dagger}$	M/F=7/5	n.a.	$28.8 \pm 1.3^{\dagger}$	$28.8 \pm 1.7^{\dagger}$	Age dependent accumulation	Negative

MMSE: Mini-Mental State Examination, HDS-R: revised Hasegawa Dementia Scale

n.a.: not available, $\dagger$ average ± standard deviation